Expansion of SARS-CoV-2-specific Antibody-secreting Cells and Generation of Neutralizing Antibodies in Hospitalized COVID-19 Patients

Running title: B cell and antibody responses in COVID-19 patients.

Authors

Renata Varnaitė[*], Marina García[*], Hedvig Glans[†,‡,1], Kimia T. Maleki[*,1], John Tyler Sandberg[*,1], Janne Tynell[*], Wanda Christ[*], Nina Lagerqvist[§], Hilmir Asgeirsson[†,¶], Hans-Gustaf Ljunggren[*,‡], Gustaf Ahlén[#], Lars Frelin[#], Matti Sällberg[#], Kim Blom[*], Jonas Klingström[*,§], Sara Gredmark-Russ[*,†]

[1] H.G., K.T.M. and J.T.S. contributed equally to this work.

Affiliations

[*] Center for Infectious Medicine, ANA Futura, Department of Medicine Huddinge, Karolinska Institutet, Stockholm, Sweden.

[†] Department of Infectious Diseases, Karolinska University Hospital, Stockholm, Sweden.

[‡] Department of Medicine Solna, Karolinska Institutet, Stockholm, Sweden.

[§] Public Health Agency of Sweden, Solna, Sweden.

[¶] Division of Infectious Diseases, Department of Medicine Huddinge, Karolinska Institutet, Stockholm, Sweden.

[#] Department of Laboratory Medicine, Division of Clinical Microbiology, ANA Futura, Karolinska Institutet, Stockholm, Sweden.

Abstract

Coronavirus disease 2019 (COVID-19), caused by severe acute respiratory syndrome coronavirus 2 (SARS-CoV-2), emerged in late 2019 and has since become a global pandemic. Pathogen-specific antibodies are typically a major predictor of protective immunity, yet B cell and antibody responses during COVID-19 are not fully understood. Here, we analyzed antibody-secreting cell (ASC) and antibody responses in twenty hospitalized COVID-19 patients. The patients exhibited typical symptoms of COVID-19, and presented with reduced lymphocyte numbers and increased T cell and B cell activation. Importantly, we detected an expansion of SARS-CoV-2 nucleocapsid protein-specific ASCs in all twenty COVID-19 patients using a multicolor FluoroSpot assay. Out of the 20 patients, 16 had developed SARS-CoV-2-neutralizing antibodies by the time of inclusion in the study. SARS-CoV-2-specific IgA, IgG and IgM antibody levels positively correlated with SARS-CoV-2-neutralizing antibody titers, suggesting that SARS-CoV-2-specific antibody levels may reflect the titers of neutralizing antibodies in COVID-19 patients during the acute phase of infection. Lastly, we showed that interleukin 6 (IL-6) and C-reactive protein (CRP) concentrations were higher in serum of patients who were hospitalized for longer, supporting the recent observations that IL-6 and CRP could be used to predict COVID-19 severity. Altogether, this study constitutes a detailed description of clinical and immunological parameters in twenty COVID-19 patients, with a focus on B cell and antibody responses, and provides tools to study immune responses to SARS-CoV-2 infection and vaccination.

Keywords: SARS-CoV-2, COVID-19, antibody-secreting cells, B cells, antibodies, T cells, interleukin 6

Introduction

Coronavirus disease 2019 (COVID-19), caused by severe acute respiratory syndrome coronavirus 2 (SARS-CoV-2), emerged in late 2019 and has since become a global pandemic (1). SARS-CoV-2 primarily affects the respiratory tract and can cause severe respiratory illness, which sometimes requires mechanical ventilation (2). The world is racing to understand the immune responses to SARS-CoV-2 in order to identify correlates of protection, and to aid treatment and vaccine development. In the majority of infections, pathogen-specific antibodies are one of the main contributors to protective immunity, yet B cell and antibody responses during COVID-19 are currently not fully understood.

B cells are one of the key players of the adaptive immune system and can provide sterilizing immunity against pathogens through the secretion of pathogen-specific antibodies. B cells carry immunoglobulin (Ig) surface receptors with a high range of specificity that can directly recognize different antigens. Early during acute infections upon the encounter with the antigen, B cells differentiate into antibody-secreting cells (ASCs), including plasmablasts and plasma cells, which produce large quantities of pathogen-specific antibodies (3).

ASCs can expand to very high levels during some acute human infections (4-7). For example, during human dengue virus infection, ASCs expand to constitute an average of 47% of all circulating B cells (5). Meanwhile, at steady state conditions in healthy individuals, ASCs comprise only up to around 1% of all circulating B cells (5). The ASC response is typically transient, peaking at around day 7 of the febrile stage of infection (8). However, during acute human respiratory syncytial virus (RSV) infection, ASC response could be detected for as long as 22-45 days after the onset of symptoms, which was found to be associated with

74 prolonged shedding of RSV in the airways (9). Thus, the kinetics of ASC response may be
75 dependent on pathogen persistence.
76
77 In humans, ASCs can be identified using flow cytometry as $CD19^{+}CD20^{low/-}$ isotype-
78 switched B cells with high cell surface expression of CD38 and CD27 molecules, as well as
79 intracellular expression of proliferation marker Ki-67 (10, 11). Although flow cytometry is a
80 valuable tool to measure the frequencies of total ASCs in peripheral blood, it only allows
81 phenotypic characterization. Functional antibody secretion capacity and antigen-specificity of
82 ASCs are typically described using the gold standard enzyme-linked immunospot (ELISpot)
83 assay (12). ELISpot is a highly sensitive method allowing for detection of ASCs producing
84 different antibody isotypes at single-cell level, including IgA, IgG and IgM, against different
85 antigens. Flow cytometry and ELISpot can therefore be used in combination to
86 comprehensively describe the magnitude and specificity of B cell responses to infectious
87 agents.
88
89 Antigen-specific antibodies can contribute to pathogen control either by (i) directly
90 interfering with the entry of a pathogen into the target cells (referred to as neutralization); or
91 by (ii) assisting the effector cells in recognizing and eliminating infected target cells (known
92 as antibody-dependent cellular cytotoxicity) (13). Neutralizing antibodies are typically
93 considered to be the strongest predictor of protective immunity following natural infection or
94 vaccination. Therefore, it is of great importance to evaluate the neutralizing capacity and
95 persistence of specific antibodies in acute viral infections such as SARS-CoV-2.
96
97 Here, we provide a detailed description of early B cell and antibody responses to SARS-CoV-
98 2 infection in a cohort of twenty hospitalized patients with severe COVID-19. We found a

substantial level of ASCs expansion in all patients, and that not all patients developed detectable levels of SARS-CoV-2-specific and neutralizing antibodies at the time of sampling. We also show increased levels of adaptive immune system activation and increased serum concentrations of inflammatory markers interleukin 6 (IL-6) and C-reactive protein (CRP), the latter two correlating with the duration of hospitalization in the present COVID-19 patient cohort. This study constitutes a detailed description of clinical and immunological B cell-related parameters in COVID-19 patients, and describes tools to study immune responses to SARS-CoV-2 infection and vaccination.

Materials and Methods

Ethics statement

The study was approved by the Regional Ethical Review Board in Stockholm, Sweden and by the Swedish Ethical Review Authority. All COVID-19 patients and healthy controls included in this study provided a written informed consent for participation.

Study subjects and sampling of peripheral blood

Peripheral blood samples were collected from 20 adult COVID-19 patients hospitalized in April 2020 at the Karolinska University Hospital in Stockholm, Sweden (5 females and 15 males; age range between 34 and 67 years; median age 53 years) (Table I). Patients were diagnosed with COVID-19 by RT-PCR for SARS-CoV-2 in either nasopharyngeal swabs (18/20 patients) or sputum (2/20 patients). Diagnostics were performed at the diagnostic laboratory at the Karolinska University Hospital, Stockholm, Sweden. Peripheral blood samples from patients were taken at a median of 15 days after self-reported onset of symptoms (range 7-19 days). Peripheral blood samples of 7 healthy controls were collected in parallel (2 females and 5 males; age range between 26 and 53 years; median age 31 years).

Peripheral blood mononuclear cells (PBMCs) were isolated from heparinized anti-coagulated blood using density gradient Lymphoprep medium (Stemcell Technologies) following the manufacturer's instructions, and immediately used for flow cytometry and FluoroSpot assays. Serum was collected from COVID-19 patients and healthy controls in BD Vacutainer serum tubes with spray-coated silica (BD Biosciences). After coagulation for up to 2 hours at RT, serum was isolated by centrifugation at 2000 *g* for 10 min and immediately stored at -80 ºC for later analysis.

134

135 ***Absolute counts of lymphocytes in peripheral blood***

136 Absolute numbers of $CD45^+$, $CD3^+$, $CD4^+$, $CD8^+$, and $CD19^+$ cells in peripheral blood were
137 measured using BD Trucount Tubes (BD Biosciences). 50 µL of anti-coagulated whole blood
138 were added into Trucount Tubes within 3 hours after blood extraction and stained with either
139 anti-CD45-PerCP (2D1), anti-CD3-FITC (SK7), anti-CD4-APC (SK3) and anti-CD8-PE
140 (SK1), or anti-CD45-PerCP (2D1) and anti-CD19-AF488 (HIB19) (all from BioLegend).
141 After 15 minutes of incubation at RT, stained whole blood was fixed and red blood cells
142 lysed with 2X BD FACS Lysing Solution (BD Biosciences). Samples were acquired on a BD
143 Accuri C6 Plus flow cytometer. Bead number recorded was used to quantify absolute $CD45^+$,
144 $CD3^+$, $CD4^+$, $CD8^+$, and $CD19^+$ cell counts per microliter of blood. ASC numbers per
145 microliter of blood were calculated based on $CD19^+$ B cell numbers measured by absolute
146 cell counting and on frequencies of ASCs within $CD19^+$ cells measured by flow cytometry.

147

148 ***Flow cytometry***

149 Staining with fluorescently-labelled antibodies was performed on freshly isolated PBMCs.
150 Briefly, cells were incubated with surface staining antibodies diluted in PBS for 30 min at
151 4°C in the dark, followed by 3 washes with flow cytometry buffer (2% FCS and 2 mM
152 EDTA in PBS). Cells were then fixed and permeabilized using eBioscience
153 Foxp3/Transcription Factor Staining Buffer Set (Thermo Fisher Scientific) and later
154 incubated with antibodies diluted in PBS for intracellular staining for 30 min at 4°C in the
155 dark. Finally, samples were incubated in a 2% formaldehyde solution (Polysciences) for 2 h,
156 washed and resuspended in flow cytometry buffer, and data subsequently acquired on a BD
157 LSRFortessa flow cytometer equipped with 355, 405, 488, 561, and 639 nm lasers and BD

158 FACSDiva Software (BD Biosciences). For a detailed gating strategy see Supplementary Fig.
159 1.
160
161 The following monoclonal antibody conjugates were used for cell surface staining: anti-CD8-
162 Qdot605 (3B5) (Thermo Fisher Scientific), anti-CD19-BUV395 (SJ25C1), anti-CD14-V500
163 (MφP9), anti-CD4 -BUV737 (RPA-T4) (all from BD Biosciences), anti-CD123-BV510
164 (6H6), anti-CD27-BV650 (O323), anti-CD20-FITC (2H7), anti-CD38-BV421 (HB-7), anti-
165 IgD-PE-Cy7 (IA6-2), anti-IgM-BV785 (MHM-88) (all from BioLegend), anti-CD3-PE-Cy5
166 (UCHT1), anti-CD56-ECD (N901) (all from Beckman Coulter), and anti-IgA-APC
167 (REA1014) (Miltenyi). LIVE/DEAD Fixable Near-IR Dead Cell Stain Kit (Thermo Fisher
168 Scientific) was used as a viability marker. The following monoclonal antibody conjugates
169 were used for intracellular staining: anti-IgG-PE (HP6017) (BioLegend) and anti-Ki-67-
170 AF700 (B56) (BD Biosciences).
171
172 ***FluoroSpot assay for antibody-secreting cells***
173 The number of SARS-CoV-2 nucleocapsid (N) protein-specific IgA, IgG and IgM antibody-
174 secreting cells (ASCs), as well as the total number of IgA-, IgG- and IgM-ASCs in freshly
175 isolated PBMCs were measured using a multicolor B cell FluoroSpot kit with modifications
176 (Mabtech). Briefly, ethanol-activated IPFL membrane plates were coated overnight with
177 either: (i) anti-IgG, anti-IgA, and anti-IgM capture antibodies (15µg/mL of each) for the
178 detection of all ASCs, or (ii) SARS-CoV-2 N protein (10 µg/mL) for the detection of SARS-
179 CoV-2-specific ASCs. The plates were washed with PBS and blocked with R10 media
180 (RPMI-1640 with 10% FCS, 1% Pen/Strep, 2mM L-Glutamine (all from Thermo Fisher
181 Scientific)) for 30 minutes at RT before the addition of freshly isolated PBMCs. Plates were
182 then incubated at 37°C in 5% CO_2 for 20 hours and then developed with anti-human IgG-550

183 (yellow fluorescence), anti-human IgA-490 (green fluorescence) and anti-human IgM-640
184 (red fluorescence) secondary detection antibodies (diluted 1:500 each) (all antibodies from
185 Mabtech). Fluorescent spots indicating a single ASC were detected with an IRIS FluoroSpot
186 reader and counted with Apex software (Mabtech).
187
188 ***Recombinant SARS-CoV-2 nucleocapsid protein***
189 A full-length nucleocapsid (N) phosphoprotein nucleotide sequence (1293 base-pairs) of the
190 SARS-CoV-2 virus was optimized and synthesized (Genscript). The synthesized sequence
191 was cloned into a PET-30a(+) vector with a carboxyterminal His tag for detection of protein
192 expression in *E.coli*. The *E. coli* strain BL21 Star (DE3) was transformed with the
193 recombinant plasmid and a single colony was inoculated into TB medium containing
194 antibiotic and cultured at 37°C at 200 rpm and then induced with IPTG. Protein purity and
195 molecular weight were determined by SDS-PAGE and Western blot according to standard
196 procedures (Genscript).
197
198 ***SARS-CoV-2 isolation from serum***
199 50 µL of serum were mixed with 150 µL of EMEM (Gibco) and added to confluent Vero E6
200 cells seeded in 24-well plates. Cells were incubated with diluted serum for 1 hour, and 1 mL
201 of Vero E6 medium was added after the incubation. Cells were subsequently incubated
202 further for 10 days at 37 °C and 5% CO_2 and monitored for cytopathic effect (CPE) by
203 optical microscopy.
204
205 ***Immunofluorescence assay (IFA) for IgG against SARS-CoV-2***
206 Vero E6 cells were infected with SARS-CoV-2 (isolate SARS-CoV-2/human/SWE/01/2020,
207 accession number MT093571) for 24 hours, trypsinized and mixed with uninfected Vero E6

208 cells, and then seeded on microscope slides. Twelve hours later, slides were fixed in acetone
209 and stored at -80˚C until further use. Serum samples were heat-inactivated at 56˚C for 30
210 minutes prior to analysis. For analysis of total SARS-CoV-2 IgG antibody titers, serum
211 samples were serially diluted from 1:20 to 1:5120. 25 µL of diluted serum was then added to
212 fixed cells and incubated at 37˚C for 30 min, after which the slides were washed in NaCl for
213 30 min. Bound SARS-CoV-2 IgG antibodies were then detected by incubating for 30 min at
214 37˚C with a secondary AF488-conjugated AffiniPure goat anti-human IgG antibody (Jackson
215 Immunoresearch), diluted 1:200 in 0.1% Evan's Blue. SARS-CoV-2 IgG positive cells were
216 visualized using a Nikon Eclipse Ni fluorescence microscope (x40 magnification). The titer
217 of IgG in each serum sample was determined by the inverted dilution factor value for the
218 highest dilution with positive staining.
219
220 ***ELISAs***
221 SARS-CoV-2 specific IgG and IgA antibodies in serum were detected using anti-SARS-
222 CoV-2 ELISA kits (both from Euroimmun), according to the manufacturer's instructions.
223 SARS-CoV-2 specific IgM antibodies were detected using EDI Novel Coronavirus COVID-
224 19 IgM ELISA kit (Epitope Diagnostics), according to the manufacturer's instructions. Serum
225 samples were heat-inactivated at 56˚C for 30 minutes prior to analysis.
226
227 IL-6 levels in serum from patients and healthy controls were measured in freshly thawed
228 serum using human IL-6 ELISA development kit (Mabtech), according to the manufacturer's
229 instructions. Serum samples were diluted 1:2 in ready-to-use ELISA diluent (Mabtech) prior
230 to performing the IL-6 ELISA assay.
231
232

233 ***Micro-neutralization assay***

234 Two-fold dilution series from 1:10 to 1:10240 in EMEM (Gibco) + 5% FCS (Thermo Fisher
235 Scientific) were performed on the serum samples, which were previously heat inactivated at
236 56˚C for 30 minutes. Each dilution was subsequently mixed with equal volume of 4000
237 $TCID_{50}$/ml SARS-CoV-2 (50 µl serum plus 50 µl virus) and incubated for 1 hour at 37 °C
238 and 5% CO_2. Each sample was prepared in duplicates. After incubation, the mixtures were
239 added on confluent Vero E6 cells seeded on 96-well plates and incubated at 37 °C 5% CO_2.
240 Four days later the cells were inspected for signs of cytopathic effect (CPE) by optical
241 microscopy. Each well was scored as either 'neutralizing' if less than 50% of the cell layer
242 showed signs of CPE, or 'non-neutralizing' if ≥50% CPE was observed. Results are shown as
243 the arithmetic mean of the reciprocals of the highest neutralizing dilutions from the two
244 duplicates for each sample.

245

246 ***Real-time RT-PCR***

247 RNA was extracted from freshly thawed serum samples using the MagDEA Dx SV reagent
248 kit and the magLEAD instrument (Precision System Science). The assay used to detect
249 SARS-CoV-2 RNA was modified from (14): forward primer 5'-
250 CATGTGTGGCGGTTCACTATATGT-3', reverse primer 5'-
251 TGTTAAARACACTATTAGCATAWGCAGT-3', and RdRp_SARSr-P2 probe. The assay
252 was carried out in 25 µL reaction mixtures containing 5µL RNA template, TaqMan Fast
253 Virus 1-Step Master Mix, 0.6 µM forward primer, 0.8 µM reverse primer, and 0.2 µM probe
254 (Applied Biosystems). Thermal cycling was performed at 50°C for 5 min, 95°C for 20 sec,
255 followed by 40 cycles of 95°C for 3 sec, and 60°C for 30 sec in a StepOne Plus real-time
256 PCR (Applied Biosystems).

257

258 ***Statistics and data analysis***

259 Statistical analyses were performed using GraphPad Prism software 7.0 for MacOSX
260 (GraphPad Software). Correlation analyses were performed using Spearman's correlation
261 test. Statistical significance for differences between COVID-19 patients and healthy controls
262 was determined by two-sided Mann-Whitney *U* test. P values of < 0.05 were considered
263 statistically significant. FlowJo software version 10.5.3 (Tree Star) was used to analyze all
264 flow cytometry data. FluoroSpot data was analyzed with Apex software (Mabtech).

265 **Results**

266 Twenty COVID-19 patients were enrolled in this study during hospitalization at Karolinska
267 University Hospital, Sweden. All twenty patients exhibited typical COVID-19 symptoms of
268 fever, cough and breathing difficulties, and a few also experienced chest pain, myalgia and
269 diarrhea (Table I). Some of the patients presented with common co-morbidities such as
270 overweightness, hypertension, asthma, cardiovascular disease and diabetes mellitus type II.
271 According to the guidelines for diagnosis and treatment of COVID-19 (Version 7) released
272 by the National Health Commission and State Administration of Traditional Chinese
273 Medicine, 19 out of the 20 patients were classified as severe, and 1 out of the 20 as critically
274 ill (15). While all patients enrolled in this study were hospitalized at the infectious diseases
275 wards at the time of sampling, two patients were treated at the intensive care unit (ICU)
276 before inclusion in this study, while one patient required ICU treatment after the inclusion.
277 Peripheral blood samples from the twenty COVID-19 patients were collected at a median of
278 15 days after the self-reported onset of symptoms, and at a median of 3 days after
279 hospitalization (Table I, Fig. 1A and B). In parallel, seven donors without an ongoing
280 respiratory disease or signs of inflammation were included in the study as healthy controls.
281

282 ***Clinical chemistry parameters in COVID-19 patients***

283 Blood cell counts and clinical chemistry parameters in peripheral blood of COVID-19
284 patients were measured at the Diagnostics Laboratory of the Karolinska University Hospital
285 on the same day as the inclusion in this study (+/– 24 hours). Clinical chemistry tests showed
286 increased levels of inflammatory markers, including C-reactive protein (CRP), lactate
287 dehydrogenase (LDH) and ferritin (Fig. 1C). Some patients also presented with increased
288 levels of aspartate transaminase (AST), alanine transaminase (ALT) and D-dimer, while
289 hemoglobin, procalcitonin (PCT) and troponin T levels fell within the range of reference

290 values in the majority of patients (Fig. 1C). Numbers of total leukocytes, neutrophils,
291 monocytes and platelets in peripheral blood were within the normal range in the majority of
292 COVID-19 patients at the time of sampling (Fig. 1C). In contrast, we observed reduced
293 lymphocyte numbers, with the median lymphocyte numbers falling below or within the lower
294 range of reference values (Fig. 1C). Reduced lymphocyte numbers in peripheral blood of
295 COVID-19 patients were confirmed by flow cytometry analysis of absolute cell counts. We
296 found significantly lower $CD45^+$ lymphocyte numbers in the patients compared to healthy
297 controls (Fig. 1D). $CD3^+$ T cell and $CD3^+CD8^+$ T cell numbers were also significantly lower
298 in patients compared to the controls, while no significant difference in the numbers of
299 $CD3^+CD4^+$ T cells and $CD19^+$ B cells was observed between COVID-19 patients and healthy
300 controls (Fig. 1D).
301
302 ***T cells and B cells are activated in COVID-19 patients***
303 We next assessed the overall activation level of the adaptive immune system in COVID-19
304 patients. T cell and B cell activation levels were measured based on the expression of the
305 activation marker CD38 and the proliferation marker Ki-67 using multicolor flow cytometry
306 on freshly isolated peripheral blood mononuclear cells (PBMCs) (Fig. 2A). We observed
307 significantly higher frequencies of activated $CD4^+$ T cells, $CD8^+$ T cells and $CD19^+$ B cells in
308 COVID-19 patients compared to healthy controls (Fig. 2B). Additionally, there was a strong
309 positive correlation between the frequencies of activated $CD8^+$ T cells and $CD4^+$ T cells in
310 COVID-19 patients ($r_s = 0.699$, $P < 0.001$) (Supplementary Fig. 2A).
311
312 ***Significant expansion of antibody-secreting cells in COVID-19 patients***
313 Flow cytometric analyses revealed increased frequencies of activated $CD38^+$Ki-67^+ B cells in
314 the COVID-19 patients (Fig. 2A and B). Therefore, we further analyzed if antibody-secreting

315 cell (ASC) frequencies were also increased in peripheral blood. ASCs were identified as
316 isotype-switched B cells expressing high levels of surface CD38 and CD27 ($CD19^{+}CD20^{low/-}$
317 $IgD^{-}CD38^{high}CD27^{high}$) (Fig. 3A). As expected, low frequencies and numbers of ASCs were
318 detected in peripheral blood of healthy controls (Fig. 3B and C). However, significantly
319 higher ASC frequencies and numbers were observed in COVID-19 patients compared to
320 healthy controls, constituting up to 31% of all circulating B cells (Fig. 3B and C).
321
322 Next, we assessed the expression of immunoglobulins (Ig) by the ASCs in COVID-19
323 patients and healthy controls (Fig. 3A). IgA has previously been shown to be expressed by
324 80% of all ASCs at steady state (16). In agreement with this, the largest proportion within the
325 ASC compartment in healthy controls was IgA^{+} ASCs, whereas the majority of ASCs in
326 COVID-19 patients expressed IgG (Fig. 3D). IgM^{+} ASCs were present at comparable
327 frequencies in both COVID-19 patients and healthy controls (Fig. 3D). Noteworthy, a
328 substantial ASC expansion was detected as early as 7 days, and as late as 19 days after the
329 onset of symptoms (Supplementary Fig. 2B).
330
331 ***Detection of SARS-CoV-2-specific antibody-secreting cells in COVID-19 patients***
332 The expansion of ASCs is usually a result of an ongoing infection and is characterized by
333 high specificity towards the infectious agent (17). To investigate if the ASCs identified by
334 flow cytometry were SARS-CoV-2-specific, we developed a FluoroSpot assay - a
335 fluorescence-based variant of the enzyme-linked immunospot (ELISpot) assay, which allows
336 for simultaneous detection of total and antigen-specific IgA-, IgG- and IgM-ASCs. To detect
337 SARS-CoV-2-specific IgA-, IgG- and IgM-ASCs, we generated recombinant SARS-CoV-2
338 nucleocapsid protein (N protein).
339

340 The FluoroSpot assay confirmed the ASC expansion detected by flow cytometry, as the total
341 numbers of IgA-, IgG-, and IgM-ASCs in COVID-19 patients were significantly higher than
342 in healthy controls (Fig. 3E and G). Moreover, the total ASC frequencies and numbers
343 detected by flow cytometry positively correlated with total numbers of ASCs measured by
344 FluoroSpot (r_s = 0.537, P = 0.01; and r_s = 0.636, P = 0.003, respectively). Consistent with
345 flow cytometry data, IgG-ASCs constituted the predominant subset of all ASCs in COVID-
346 19 patients, followed by IgA-ASCs (Fig. 3D and G).
347
348 Importantly, we detected SARS-CoV-2 N protein-specific ASCs in all twenty COVID-19
349 patients, but not in controls, suggesting an active SARS-CoV-2-specific B cell response in
350 acute COVID-19 (Fig. 3F and H). We detected IgA-, IgG- and IgM-ASCs that are specific
351 for SARS-CoV-2 N-protein, yet at highly variable numbers among the patients. Overall, N-
352 protein-specific ASCs constituted a small fraction of total ASCs [median (IQR) = 3.47%
353 (2.5-4.9)]. Nonetheless, total ASC frequencies determined by flow cytometry positively
354 correlated with N protein-specific ASC numbers (r_s = 0.574, P = 0.008), suggesting that the
355 ASC expansion detected by flow cytometry may reflect the magnitude of SARS-CoV-2 N
356 protein-specific ASC response.
357
358 ***Generation of SARS-CoV-2-specific and neutralizing antibodies in COVID-19 patients***
359 The expansion of SARS-CoV-2-specific ASCs in all of the patients in our cohort suggested
360 that the patients had developed SARS-CoV-2-specific antibodies in response to the infection.
361 To investigate this in detail, we next analyzed SARS-CoV-2-specific antibody levels.
362
363 First, we measured SARS-CoV-2 spike S1-specific IgA and IgG, as well as N-protein-
364 specific IgM antibody levels by ELISAs. We found detectable SARS-CoV-2-specific IgA

365 (15/20 patients), IgG (15/20 patients) and IgM (16/20 patients) antibody levels in most of the
366 COVID-19 patients (Fig. 4A and B). Next, we determined total anti-SARS-CoV-2 IgG
367 antibody levels measured towards SARS-CoV-2-infected cells using an immunofluorescence
368 assay (IFA) (Fig. 4C). We found that 16 out of the 20 patients were positive in this assay,
369 with titers ranging from 40 to 5120 (Fig. 4C). As expected, none of the healthy controls were
370 positive in any of the antibody assays (Fig. 4A). Higher IgG levels were detected in patients
371 who were sampled late compared to early after the onset of symptoms, as total and spike S1-
372 specific SARS-CoV-2 IgG antibody levels positively correlated with the number of days
373 since symptom onset ($r_s = 0.577$, $P = 0.01$, and $r_s = 0.603$, $P = 0.005$, respectively)
374 (Supplementary Fig. 2C and D).
375
376 Next, using a micro-neutralization assay we assessed if the COVID-19 patients had generated
377 SARS-CoV-2-neutralizing antibodies (18). This assay measures the ability of COVID-19
378 patient serum to reduce the cytopathic effect (CPE) caused by SARS-CoV-2 infection of
379 susceptible cells *in vitro*. Neutralizing antibodies were detected in most of the patients
380 (16/20), but at heterogeneous titers ranging from 10 to 1920 (Fig. 4D). Three of the four
381 patients with undetectable levels of SARS-CoV-2-neutralizing antibodies were also below
382 the level of detection for SARS-CoV-2-specific antibodies in IFA and all ELISAs (Fig. 4A).
383
384 Interestingly, we observed a strong positive correlation between total SARS-CoV-2-specific
385 IgG antibody levels and neutralizing antibody titers in COVID-19 patients (Fig. 4E). Both
386 S1-specific IgA and IgG, as well as N-specific IgM levels also correlated with SARS-CoV-2-
387 neutralizing antibody titers suggesting that SARS-CoV-2-specific antibody titers may reflect
388 the levels of neutralizing antibodies during the acute phase of COVID-19 (Fig. 4E).
389

390 Next, we assessed if the frequencies of activated T cells and B cells correlate with SARS-
391 CoV-2-neutralizing antibody responses. We found that $CD8^+$ T cell activation level, but not
392 $CD4^+$ T cell or $CD19^+$ B cell activation level, positively correlated with neutralizing antibody
393 titers ($r_s = 0.544$, P = 0.01; $r_s = 0.271$, P = 0.25, and $r_s = -0.136$, P = 0.57, respectively)
394 (Supplementary Fig. 2E - G).
395
396 ***Detection of SARS-CoV-2 RNA in serum of COVID-19 patients***
397 An important role of neutralizing antibodies is to limit the spread of the virus. We screened
398 all serum samples by real time RT-PCR for SARS-CoV-2 RNA (14). Three COVID-19
399 patients were positive for SARS-CoV-2 RNA in serum (Fig. 4A). Notably, 2 out of the 3
400 SARS-CoV-2 RT-PCR-positive patients lacked detectable levels of neutralizing antibodies,
401 which might allow for a more efficient spread of SARS-CoV-2 in those patients (Fig. 4A).
402 However, our attempts to isolate live SARS-CoV-2 from patient serum on Vero E6 cells were
403 unsuccessful (data not shown), suggesting absence or low levels of live SARS-CoV-2 in
404 serum of COVID-19 patients.
405
406 ***Inflammatory makers, neutralizing antibodies and disease severity in COVID-19***
407 The pro-inflammatory cytokine IL-6 and CRP serum levels have been shown to correlate
408 with disease severity in COVID-19 patients (19, 20). We measured IL-6 serum concentration
409 in all COVID-19 patients at the time of inclusion in this study using ELISA. We found
410 heterogenous, yet significantly higher median concentration of IL-6 in COVID-19 patients
411 compared to the controls (Fig. 5A).
412
413 There was a strong positive correlation between the IL-6 and CRP levels at the time of
414 inclusion in this study (Fig. 5B). Higher serum concentrations of both IL-6 and CRP were

415 higher in patients with longer duration of hospitalization (Fig. 5B). Notably, IL-6 and CRP
416 serum concentrations negatively correlated with neutralizing antibody titers in COVID-19
417 patients, indicating a possible link between inflammation and humoral responses in COVID-
418 19 (Fig. 5B).
419
420

421 **Discussion**

422 Here, we demonstrated that COVID-19 patients elicit a SARS-CoV-2-specific B cell
423 response, indicated by the expansion of SARS-CoV-2-specific ASCs. Although not all
424 patients in the present cohort had detectable levels of SARS-CoV-2-specific antibodies at the
425 time of sampling, SARS-CoV-2 nucleocapsid protein-specific ASCs could be detected in all
426 patients using the FluoroSpot assay. In addition, we showed a clear relationship between the
427 levels of SARS-CoV-2-specific antibodies and total SARS-CoV-2-neutralizing antibodies.
428 This suggests that standard serological assays may inform about the levels of neutralizing
429 SARS-CoV-2-specific antibodies, which may offer protection from a re-infection.
430 Additionally, tools employed in this study may be of relevance in the assessment of long-
431 lasting immunity after SARS-CoV-2 infection and vaccination.

432

433 The expansion of ASCs in the present cohort of COVID-19 patients highlights an active B
434 cell response to SARS-CoV-2 infection. The frequencies of ASCs within the total circulating
435 B cell population were highly variable between COVID-19 patients, ranging from 3 to 31%.
436 Although the patients in this cohort were sampled at different timepoints following the onset
437 of symptoms, a high variability in ASC frequencies have also been observed among patients
438 infected with influenza or dengue virus sampled at normalized timepoints (e.g., 7 days after
439 febrile illness) (4, 5). Although ASCs have been shown to expand to very high levels in some
440 viral infections, constituting up to 50-80% of all peripheral B cells, the highest ASCs
441 frequency in this cohort of COVID-19 patients was 31% (5, 7, 21). Healthy controls in this
442 study had very low frequencies of ASCs in the circulation, a finding consistent with previous
443 observations (5, 6, 16).

444

445 The ASC response in peripheral blood is usually transient and peak at around 7 days after the
446 onset of febrile illness, dropping to steady-state levels 2-3 weeks later (8). Interestingly, we
447 observed a substantial ASC expansion as late as 19 days following symptom debut. This
448 finding highlights the similarity between COVID-19 and respiratory syncytial virus (RSV)
449 infection, where a significant ASC expansion could be detected as late as 22-45 days after the
450 onset of symptoms (9). The prolonged ASC expansion in RSV infection was associated with
451 longer RSV shedding in the airways. Thus, the kinetics of ASC response may be dependent
452 on pathogen persistence. In support of our findings, a recent report on longitudinal immune
453 responses in a single COVID-19 patient with mild disease showed the peak of ASC
454 expansion at day 8 after symptom onset, but a substantial ASCs response could still be
455 detected by day 20 (22). Thus, it remains to be investigated whether SARS-CoV-2
456 persistence in the airways may lead to a prolonged ASC response in circulation.
457
458 The expansion of ASCs is usually characterized by high specificity towards the infectious
459 agent (17). Here, we successfully demonstrated that COVID-19 patients generate SARS-
460 CoV-2-specific ASC responses using a FluoroSpot assay. We were able to successfully
461 identify SARS-CoV-2-specific IgA-, IgG- and IgM-ASCs in all COVID-19 patients. The
462 frequency of SARS-CoV-2-specific ASCs within the total ASC population in this patient
463 cohort was relatively low. However, since only the SARS-CoV-2 N protein was used to
464 detect specific ASCs in this study, the numbers of N protein-specific ASCs do not reflect the
465 overall magnitude of the specific ASC response. The use of SARS-CoV-2 viral lysate or
466 recombinant SARS-CoV-2 proteins in combination would allow for the evaluation of the
467 overall ASC response. Furthermore, the FluoroSpot assay described in this study could be
468 adapted to evaluate memory B cell responses to various SARS-CoV-2 proteins in
469 convalescent COVID-19 patient samples.

470

471 The protective level of SARS-CoV-2-neutralizing antibodies in COVID-19 has not yet been
472 determined. Monoclonal antibodies isolated from convalescent COVID-19 patients showed a
473 strong SARS-CoV-2-neutralizing capacity *in vitro* and *in vivo* in transgenic mice expressing
474 human SARS-CoV-2 receptor ACE2 (23). However, extensive longitudinal studies in
475 humans are required to investigate if recovered COVID-19 patients are protected from re-
476 infection with SARS-CoV-2. Seroconversion in COVID-19 patients, measured by detectable
477 SARS-CoV-2-specific IgG levels, has been recently shown to take place within nineteen days
478 after the onset of symptoms (24). The four patients in the present COVID-19 cohort without
479 detectable neutralizing antibody titers were sampled at days 7, 8, 9, and 15 after symptom
480 debut. Although these four patients did not have detectable neutralizing antibody titers,
481 SARS-CoV-2 specific ASCs were detected. This indicates that the FluoroSpot assay may be
482 a more sensitive method to detect early B cell responses to SARS-CoV-2, compared to
483 standard serological assays.

484

485 In this cohort of patients, 2 out of the 4 patients with undetectable neutralizing antibody
486 levels had SARS-CoV-2 RNA in serum. Currently, the extent to which neutralizing
487 antibodies contribute to the control of viremia in COVID-19 is unclear. Our results seem to
488 suggest that neutralizing antibodies may not be the only player in SARS-CoV-2 control in
489 circulation, as one patient with substantial levels of SARS-CoV-2-neutralizing antibodies in
490 this cohort had detectable serum levels of SARS-CoV-2 RNA. A pilot study assessing the
491 effectiveness of COVID-19 patient treatment with convalescent plasma containing SARS-
492 CoV-2-neutralizing antibodies found that the treatment reduced viral load in patients within a
493 few days after administration, suggesting that neutralizing antibodies have a role in the
494 management of viremia in COVID-19 (25).

495

496 Rapid serology tests are essential for COVID-19 diagnostics and for national serosurveillance
497 programs. Neutralizing antibody tests, however, are usually laborious and time-consuming.
498 Therefore, diagnostic tests often rely on other methods such as ELISA. Antibody levels
499 detected by ELISA, however, do not necessarily reflect the neutralization capacity of patient
500 serum. Here, we demonstrated a strong correlation between SARS-CoV-2-specific and
501 SARS-CoV-2-neutralizing antibody titers. These data suggest that the levels of SARS-CoV-
502 2-specific antibodies measured with ELISA may reflect the capacity of serum from COVID-
503 19 patients to neutralize SARS-CoV-2.

504

505 COVID-19 patients generally present with decreased lymphocyte numbers in peripheral
506 blood, which is particularly pronounced in severe cases (19, 26, 27). T cells appear to be the
507 most affected lymphocyte subset. In agreement with these observations, we found decreased
508 numbers of lymphocytes, and significantly lower T cell numbers in the present cohort of
509 COVID-19 patients.

510

511 In addition to lymphopenia, COVID-19 patients typically display increased concentrations of
512 inflammatory cytokines in serum, especially in severe cases (19, 27). The levels of
513 inflammatory markers IL-6 and CRP, in particular, have been shown to correlate with disease
514 severity in COVID-19 patients (19, 20). In this cohort of COVID-19 patients we also
515 observed increased levels of IL-6 and CRP, with comparable median values to those
516 measured by Liu *et al*. in severe COVID-19 patients (20). We show that higher IL-6 and CRP
517 levels were observed in patients who were hospitalized for longer, suggesting that these
518 markers may be of use in predicting the duration of COVID-19.

519

520 Lastly, we observed an inverse correlation between IL-6 levels and SARS-CoV-2-
521 neutralizing antibody titers in COVID-19 patients. This relationship may indicate that the
522 lack of SARS-CoV-2-neutralizing antibodies leads to higher inflammation, or that high levels
523 of inflammation impair or delay antibody responses. Further studies where a longitudinal
524 patient sampling at controlled timepoints is performed are required to describe the
525 relationship between inflammation and humoral responses in COVID-19.
526
527 Taken together, we provided a detailed description of clinical and immunological parameters
528 in twenty COVID-19 patients, with a focus on B cell and antibody responses. We
529 demonstrated that COVID-19 patients elicit a SARS-CoV-2-specific B cell response,
530 indicated by the expansion of SARS-CoV-2-specific ASCs. In addition, we showed a clear
531 relationship between the levels of SARS-CoV-2-specific antibodies and total SARS-CoV-2-
532 neutralizing antibodies. The tools employed in this study may be of relevance in the
533 assessment of long-lasting immunity after SARS-CoV-2 infection and vaccination.
534
535
536

537 **Conflict of interest**

538 Authors declare no conflicts of interest.

539

540 **Acknowledgments**

541 We would like to thank the patients and healthy controls for participating in the study. We
542 thank the nurses at the Karolinska University Hospital, Stockholm, Sweden for blood
543 sampling of patients, T. Aktas and M. Olausson at the Public Health Agency of Sweden for
544 technical assistance, and P. Schierloh at IBB-UNER-CONICET (Argentina) for providing
545 input on statistical analysis.

546 **References**

547 1. Zhou, P., X.-L. Yang, X.-G. Wang, Ben Hu, L. Zhang, W. Zhang, H.-R. Si, Y. Zhu, B. Li,
548 C.-L. Huang, H.-D. Chen, J. Chen, Y. Luo, H. Guo, R.-D. Jiang, M.-Q. Liu, Y. Chen, X.-R.
549 Shen, X. Wang, X.-S. Zheng, K. Zhao, Q.-J. Chen, F. Deng, L.-L. Liu, B. Yan, F.-X. Zhan,
550 Y.-Y. Wang, G.-F. Xiao, and Z.-L. Shi. 2020. A pneumonia outbreak associated with a new
551 coronavirus of probable bat origin. *Nature* 579: 270–273.

552 2. Huang, C., Y. Wang, X. Li, L. Ren, J. Zhao, Y. Hu, L. Zhang, G. Fan, J. Xu, X. Gu, Z.
553 Cheng, T. Yu, J. Xia, Y. Wei, W. Wu, X. Xie, W. Yin, H. Li, M. Liu, Y. Xiao, H. Gao, L.
554 Guo, J. Xie, G. Wang, R. Jiang, Z. Gao, Q. Jin, J. Wang, and B. Cao. 2020. Clinical features
555 of patients infected with 2019 novel coronavirus in Wuhan, China. *Lancet* 395: 497–506.

556 3. Nutt, S. L., P. D. Hodgkin, D. M. Tarlinton, and L. M. Corcoran. 2015. The generation of
557 antibody-secreting plasma cells. *Nat Immunol* 15: 160–171.

558 4. Huang, K.-Y. A., C. K.-F. Li, E. Clutterbuck, C. Chui, T. Wilkinson, A. Gilbert, J. Oxford,
559 R. Lambkin-Williams, T.-Y. Lin, A. J. McMichael, and X.-N. Xu. 2014. Virus-Specific
560 Antibody Secreting Cell, Memory B-cell, and Sero-Antibody Responses in the Human
561 Influenza Challenge Model. *J. Infect. Dis.* 209: 1354–1361.

562 5. Wrammert, J., N. Onlamoon, R. S. Akondy, G. C. Perng, K. Polsrila, A. Chandele, M.
563 Kwissa, B. Pulendran, P. C. Wilson, O. Wittawatmongkol, S. Yoksan, N. Angkasekwinai, K.
564 Pattanapanyasat, K. Chokephaibulkit, and R. Ahmed. 2012. Rapid and massive virus-specific
565 plasmablast responses during acute dengue virus infection in humans. *J. Virol.* 86: 2911–
566 2918.

567 6. García, M., A. Iglesias, V. I. Landoni, C. Bellomo, A. Bruno, M. T. Córdoba, L. Balboa,
568 G. C. Fernández, M. D. C. Sasiain, V. P. Martínez, and P. Schierloh. 2017. Massive
569 plasmablast response elicited in the acute phase of hantavirus pulmonary syndrome.
570 *Immunology* 151: 122–135.

571 7. McElroy, A. K., R. S. Akondy, C. W. Davis, A. H. Ellebedy, A. K. Mehta, C. S. Kraft, G.
572 M. Lyon, B. S. Ribner, J. Varkey, J. Sidney, A. Sette, S. Campbell, U. Ströher, I. Damon, S.
573 T. Nichol, C. F. Spiropoulou, and R. Ahmed. 2015. Human Ebola virus infection results in
574 substantial immune activation. *Proc. Natl. Acad. Sci. U.S.A.* 112: 4719–4724.
575 8. Fink, K. 2012. Origin and function of circulating plasmablasts during acute viral
576 infections. *Front Immunol* 3: 1–5.
577 9. Lee, F. E.-H., A. R. Falsey, J. L. Halliley, I. Sanz, and E. E. Walsh. 2010. Circulating
578 antibody-secreting cells during acute respiratory syncytial virus infection in adults. *J. Infect.*
579 *Dis.* 202: 1659–1666.
580 10. Wrammert, J., K. Smith, J. Miller, W. A. Langley, K. Kokko, C. Larsen, N.-Y. Zheng, I.
581 Mays, L. Garman, C. Helms, J. James, G. M. Air, J. D. Capra, R. Ahmed, and P. C. Wilson.
582 2008. Rapid cloning of high-affinity human monoclonal antibodies against influenza virus.
583 *Nature* 453: 667–671.
584 11. Qian, Y., C. Wei, F. Eun-Hyung Lee, J. Campbell, J. Halliley, J. A. Lee, J. Cai, Y. M.
585 Kong, E. Sadat, E. Thomson, P. Dunn, A. C. Seegmiller, N. J. Karandikar, C. M. Tipton, T.
586 Mosmann, I. Sanz, and R. H. Scheuermann. 2010. Elucidation of seventeen human peripheral
587 blood B-cell subsets and quantification of the tetanus response using a density-based method
588 for the automated identification of cell populations in multidimensional flow cytometry data.
589 *Cytometry B Clin Cytom* 78: S69–82.
590 12. Crotty, S., R. D. Aubert, J. Glidewell, and R. Ahmed. 2004. Tracking human antigen-
591 specific memory B cells: a sensitive and generalized ELISPOT system. *J. Immunol. Methods*
592 286: 111–122.
593 13. Murin, C. D., I. A. Wilson, and A. B. Ward. 2019. Antibody responses to viral infections:
594 a structural perspective across three different enveloped viruses. *Nature Microbiology* 4:
595 734–747.

596 14. Corman, V. M., O. Landt, M. Kaiser, R. Molenkamp, A. Meijer, D. K. Chu, T. Bleicker,
597 S. Brünink, J. Schneider, M. L. Schmidt, D. G. Mulders, B. L. Haagmans, B. van der Veer, S.
598 van den Brink, L. Wijsman, G. Goderski, J.-L. Romette, J. Ellis, M. Zambon, M. Peiris, H.
599 Goossens, C. Reusken, M. P. Koopmans, and C. Drosten. 2020. Detection of 2019 novel
600 coronavirus (2019-nCoV) by real-time RT-PCR. *Euro Surveill.* 25: 2431.
601 15. National Health Commission State Administration of Traditional Chinese Medicine.
602 2020. Diagnosis and Treatment Protocol for Novel Coronavirus Pneumonia (Trial Version 7).
603 16. Mei, H. E., T. Yoshida, W. Sime, F. Hiepe, K. Thiele, R. A. Manz, A. Radbruch, and T.
604 Doerner. 2009. Blood-borne human plasma cells in steady state are derived from mucosal
605 immune responses. *Blood* 113: 2461–2469.
606 17. Lee, F. E. H., J. L. Halliley, E. E. Walsh, A. P. Moscatiello, B. L. Kmush, A. R. Falsey,
607 T. D. Randall, D. A. Kaminiski, R. K. Miller, and I. Sanz. 2011. Circulating Human
608 Antibody-Secreting Cells during Vaccinations and Respiratory Viral Infections Are
609 Characterized by High Specificity and Lack of Bystander Effect. *J. Immunol.* 186: 5514–
610 5521.
611 18. Manenti, A., M. Maggetti, E. Casa, D. Martinuzzi, A. Torelli, C. M. Trombetta, S.
612 Marchi, and E. Montomoli. 2020. Evaluation of SARS-CoV-2 neutralizing antibodies using a
613 CPE-based colorimetric live virus micro-neutralization assay in human serum samples. *J.*
614 *Med. Virol.* 38: 1.
615 19. Zhang, X., Y. Tan, Y. Ling, G. Lu, F. Liu, Z. Yi, X. Jia, M. Wu, B. Shi, S. Xu, J. Chen,
616 W. Wang, B. Chen, L. Jiang, S. Yu, J. Lu, J. Wang, M. Xu, Z. Yuan, Q. Zhang, X. Zhang, G.
617 Zhao, S. Wang, S. Chen, and H. Lu. 2020. Viral and host factors related to the clinical
618 outcome of COVID-19. *Nature* 1–7.

619 20. Liu, F., L. Li, M. Xu, J. Wu, D. Luo, Y. Zhu, B. Li, X. Song, and X. Zhou. 2020.
620 Prognostic value of interleukin-6, C-reactive protein, and procalcitonin in patients with
621 COVID-19. *J. Clin. Virol.* 127: 104370.
622 21. Garcia-Bates, T. M., M. T. Cordeiro, E. J. M. Nascimento, A. P. Smith, K. M. Soares de
623 Melo, S. P. McBurney, J. D. Evans, E. T. A. Marques, and S. M. Barratt-Boyes. 2013.
624 Association between magnitude of the virus-specific plasmablast response and disease
625 severity in dengue patients. *J. Immunol.* 190: 80–87.
626 22. Thevarajan, I., T. H. O. Nguyen, M. Koutsakos, J. Druce, L. Caly, C. E. Sandt, X. Jia, S.
627 Nicholson, M. Catton, B. Cowie, S. Y. C. Tong, S. R. Lewin, and K. Kedzierska. 2020.
628 Breadth of concomitant immune responses prior to patient recovery: a case report of non-
629 severe COVID-19. *Nat. Med.* 1–10.
630 23. Cao, Y., B. Su, X. Guo, W. Sun, Y. Deng, L. Bao, Q. Zhu, X. Zhang, Y. Zheng, C. Geng,
631 X. Chai, R. He, X. Li, Q. Lv, H. Zhu, W. Deng, Y. Xu, Y. Wang, L. Qiao, Y. Tan, L. Song,
632 G. Wang, X. Du, N. Gao, J. Liu, J. Xiao, X.-D. Su, Z. Du, Y. Feng, C. Qin, C. Qin, R. Jin,
633 and X. S. Xie. 2020. Potent neutralizing antibodies against SARS-CoV-2 identified by high-
634 throughput single-cell sequencing of convalescent patients' B cells. *Cell* 183: 1–12.
635 24. Long, Q.-X., B.-Z. Liu, H.-J. Deng, G.-C. Wu, K. Deng, Y.-K. Chen, P. Liao, J.-F. Qiu,
636 Y. Lin, X.-F. Cai, D.-Q. Wang, Y. Hu, J.-H. Ren, N. Tang, Y.-Y. Xu, L.-H. Yu, Z. Mo, F.
637 Gong, X.-L. Zhang, W.-G. Tian, L. Hu, X.-X. Zhang, J.-L. Xiang, H.-X. Du, H.-W. Liu, C.-
638 H. Lang, X.-H. Luo, S.-B. Wu, X.-P. Cui, Z. Zhou, M.-M. Zhu, J. Wang, C.-J. Xue, X.-F. Li,
639 L. Wang, Z.-J. Li, K. Wang, C.-C. Niu, Q.-J. Yang, X.-J. Tang, Y. Zhang, X.-M. Liu, J.-J. Li,
640 D.-C. Zhang, F. Zhang, P. Liu, J. Yuan, Q. Li, J.-L. Hu, J. Chen, and A.-L. Huang. 2020.
641 Antibody responses to SARS-CoV-2 in patients with COVID-19. *Nat. Med.* 1–15.
642 25. Duan, K., B. Liu, C. Li, H. Zhang, T. Yu, J. Qu, M. Zhou, L. Chen, S. Meng, Y. Hu, C.
643 Peng, M. Yuan, J. Huang, Z. Wang, J. Yu, X. Gao, D. Wang, X. Yu, L. Li, J. Zhang, X. Wu,

644 B. Li, Y. Xu, W. Chen, Y. Peng, Y. Hu, L. Lin, X. Liu, S. Huang, Z. Zhou, L. Zhang, Y.
645 Wang, Z. Zhang, K. Deng, Z. Xia, Q. Gong, W. Zhang, X. Zheng, Y. Liu, H. Yang, D. Zhou,
646 D. Yu, J. Hou, Z. Shi, S. Chen, Z. Chen, X. Zhang, and X. Yang. 2020. Effectiveness of
647 convalescent plasma therapy in severe COVID-19 patients. *Proc. Natl. Acad. Sci. U.S.A.* 117:
648 9490–9496.
649 26. Wang, F., J. Nie, H. Wang, Q. Zhao, and Y. X. 2020. Characteristics of Peripheral
650 Lymphocyte Subset Alteration in COVID-19 Pneumonia. *J. Infect. Dis.* 221: 1762–1769.
651 27. Qin, C., L. Zhou, Z. Hu, S. Zhang, S. Yang, Y. Tao, C. Xie, K. Ma, K. Shang, W. Wang,
652 and D.-S. Tian. 2020. Dysregulation of immune response in patients with COVID-19 in
653 Wuhan, China. *Clin. Infect. Dis.* 1-7
654
655

656 **Footnotes**

657 **1. Grant support**

658 This work was supported by the Marianne and Marcus Wallenberg Foundation (SGR), and

659 the KID PhD student funding program from Karolinska Institutet (SGR), the Swedish

660 Research Council (JK), and the SciLifeLab national COVID-19 research program (JK).

661

662 **2. Abbreviations**

663 ASC – antibody-secreting cell

664 CPE – cytopathic effect

665 COVID-19 – coronavirus disease 2019

666 N protein – nucleocapsid protein

667 SARS-CoV-2 – severe acute respiratory syndrome coronavirus 2

668 S1 protein – subunit 1 of SARS-CoV-2 spike protein

669

670 **3. Corresponding author**

671 Sara Gredmark-Russ, Center for Infectious Medicine, ANA Futura, Department of Medicine,

672 Karolinska Institutet, Karolinska University Hospital Huddinge, 141 52 Stockholm, Sweden,

673 Telephone: +46 8 58589688, Fax: +46 8 7467637, E-mail: sara.gredmark.russ@ki.se

674

675

676

677

678 **Figure legends**

679 **Figure 1. Clinical chemistry parameters in peripheral blood of COVID-19 patients.**
680 (A) Number of days since the onset of COVID-19 symptoms that peripheral blood samples
681 were taken. (B) Number of days since hospitalization that peripheral blood samples were
682 taken. (C) Blood cell counts and clinical chemistry parameters in peripheral blood of
683 COVID-19 patients measured on the day of the inclusion in this study (+/– 24 hours). Gray
684 boxes indicate the range for reference values. (D) Absolute numbers of $CD45^+$, $CD3^+$, $CD4^+$,
685 $CD8^+$, and $CD19^+$ cells in peripheral blood of COVID-19 patients (n = 20) and healthy
686 controls (HC) (n = 7) measured by flow cytometry. Statistical significance was determined
687 using Mann-Whitney *U* test (D). Graphs display median and IQR. n = number of patients.
688 CRP – C-reactive protein; LDH – lactate dehydrogenase; AST – aspartate transaminase; ALT
689 – alanine transaminase; PCT – procalcitonin; DL – detection limit. *, $P < 0.05$; **, $P < 0.01$;
690 ***, $P < 0.001$; ns – not significant.

691

692 **Figure 2. T cells and B cells are activated in peripheral blood of COVID-19 patients.**
693 (A) Representative flow cytometry plots of CD38 and Ki-67 co-expression in $CD4^+$ and
694 $CD8^+$ T cells, as well as $CD19^+$ B cells in one representative COVID-19 patient (16 days
695 after symptom onset) and one healthy control (HC). (B) Frequencies of CD38 and Ki-67 co-
696 expressing $CD4^+$ T cells, $CD8^+$ T cells and $CD19^+$ B cells in COVID-19 patients (n = 20) and
697 healthy donors (n = 7). Bar graphs display median and IQR. Statistical significance was
698 determined using Mann-Whitney *U* test. *, $P < 0.05$; ***, $P < 0.001$.

699

700 **Figure 3. SARS-CoV-2 nucleocapsid protein-specific antibody-secreting cells (ASCs)**
701 **expand in COVID-19 patients.** (A) Flow cytometry gating strategy used to identify ASCs
702 and the IgA-, IgG-, and IgM-ASC subsets. B cells are gated on live $CD14^-CD123^-CD3^-CD4^-$

703 cells. (B) Frequencies of ASCs within all B cells in COVID-19 patients and in HCs. ASCs
704 were defined as $CD19^{+}CD20^{low/-}IgD^{-}CD38^{high}CD27^{high}$. (C) Numbers of ASCs per microliter
705 of whole blood, calculated using absolute B cell numbers and frequencies of ASCs measured
706 by flow cytometry. (D) Frequencies of IgA-, IgG-, and IgM-ASCs within the total ASC
707 population measured by flow cytometry. (E and F) Representative images of wells from a
708 FluoroSpot assay showing total IgA-, IgG-, and IgM-ASCs (E), and SARS-CoV-2
709 nucleocapsid protein-specific ASCs (F) from one COVID-19 patient (13 days after symptom
710 onset) and one healthy control. IgM fluorescence is originally red, but replaced with white in
711 this figure for visualization purpose. (G) Numbers of total IgA-, IgG-, and IgM-ASCs per
712 million PBMCs, as measured by FluoroSpot assay. (H) Numbers of SARS-CoV-2
713 nucleocapsid protein-specific IgA-, IgG-, and IgM-ASCs per million PBMCs. Experiments
714 were performed on all COVID-19 patients (n = 20) and healthy controls (n = 7). Statistical
715 significance was determined using Mann-Whitney *U* test (B, C, D and G). Bar graphs display
716 median and IQR. **, $P < 0.01$; ***, $P < 0.001$; ns – not significant.
717
718 **Figure 4. SARS-CoV-2-specific and neutralizing antibody levels in COVID-19 patients.**
719 (A) Individual antibody responses to SARS-CoV-2 in COVID-19 patients (n = 20) and
720 healthy controls (HC) (n = 7). Positivity for IgA against S1-protein, IgG against S1-protein,
721 IgM against N protein, total IgG antibodies against whole SARS-CoV-2, and SARS-CoV-2-
722 neutralizing antibody titers are presented in the heatmap. Blue color indicates a positive
723 response and the color scale is adjusted for the minimum positive assay value and the highest
724 value recorded within the patient cohort for each assay. White boxes indicate values below
725 positive threshold or below detection level for each assay. Red asterisks represent patients
726 with detectable levels of SARS-CoV-2 RNA in serum. (B) IgA, IgG, and IgM antibody levels
727 in COVID-19 patients and controls, analyzed by ELISAs. Dotted horizontal line indicates the

728 threshold for positive result. OD, optical density. OD ratio = OD of the sample divided by
729 OD of the calibrator. (C) Total SARS-CoV-2 IgG antibody titers determined by
730 immunofluorescence assay. Patients with titers < 20 were assigned a value of 1. (D) SARS-
731 CoV-2-neutralizing antibody titers determined by microneutralization assay. Patients with
732 titers < 10 were assigned a value of 1. (E) Correlation between SARS-CoV-2-specific IgA,
733 IgG and IgM antibody titers and SARS-CoV-2-neutralizing antibody titers, tested with
734 Spearman's correlation test. r_s: Spearman's rank correlation coefficient. $P < 0.05$ was
735 considered statistically significant. Four data points from COVID-19 patients with identical
736 values are highlighted (5, 7, 10 and 13). Bar graphs display median and IQR.
737
738 **Figure 5. Correlations between the levels of IL-6, CRP, neutralizing antibodies and the**
739 **duration of COVID-19.** (A) Serum concentrations of IL-6 in COVID-19 patients and
740 healthy controls. Bar graph displays median and IQR. Statistical significance was determined
741 using Mann-Whitney *U* test. (B) Correlation matrix for serum IL-6, CRP, neutralizing
742 antibody titers, duration of hospitalization and the number of days between symptom onset to
743 discharge from hospital. Correlations were examined by Spearman's correlation test. The
744 color scale represents the range values for Spearman's rank correlation coefficient (r_s). *, $P <$
745 0.05; **, $P < 0.01$; ***, $P < 0.001$.

Table I. Clinical characteristics of 20 hospitalized COVID-19 patients.

Cohort characteristics	
Age, years, median (range)	53 (34-67)
Male, n (%)	15 (75)
Symptom onset to sampling, days, median (range)	15 (7-19)
Hospitalization to sampling, days, median (range)	3 (2-10)
Symptom onset to discharge, days, median (range)	19.5 (9-30)
Duration of hospitalization, days, median (range)	7.5 (3-25)
Intensive care unit (ICU) treatment[a], n (%)	3 (15)
Fatal outcome, n (%)	1 (5)
Comorbidities	**n (%)**
Overweight (BMI >25), n/N (%)	14/14 (100)[b]
Diabetes mellitus type II	4 (20)
Hypertension	3 (15)
Asthma	2 (10)
Cardiovascular disease	1 (5)
Symptoms	**n (%)**
Fever (>38°C)	20 (100)
Cough	20 (100)
Respiratory difficulties ($SpO_2 \leq 93\%$ on room air)	20 (100)
Myalgia	9 (45)
Chest pain	6 (30)
Diarrhea	4 (20)
Treatment	**n (%)**
Supplemental oxygen[c]	20 (100)
High flow nasal oxygen	4 (20)
Inhaled bronchodilators	2 (10)
Low molecular weight heparin	17 (85)
Antibiotics	14 (70)
Immunomodulatory drugs[d] (given before sampling)	3 (15)

Abbreviations: n: number of patients; BMI: body mass index. SpO_2: percutaneous oxygen saturation.

[a] ICU treatment before study sampling (n=2), ICU treatment after study sampling (n=1).
[b] n/N (%), where N is the total number of patients with available data.
[c] Oxygen flow rate – minimum 2.5 L/min. 1 patient in mechanical ventilation.
[d] Chloroquine phosphate (n=2) or Anakinra (n=1).

Figure 1 Varnaite et al.

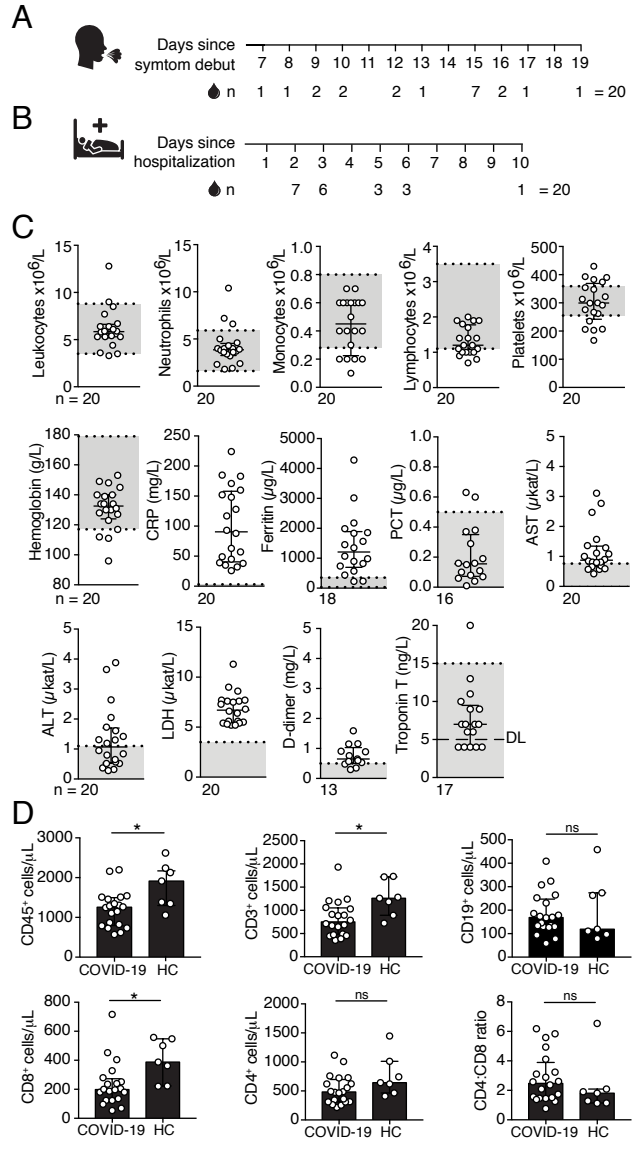

Figure 2 Varnaite et al.

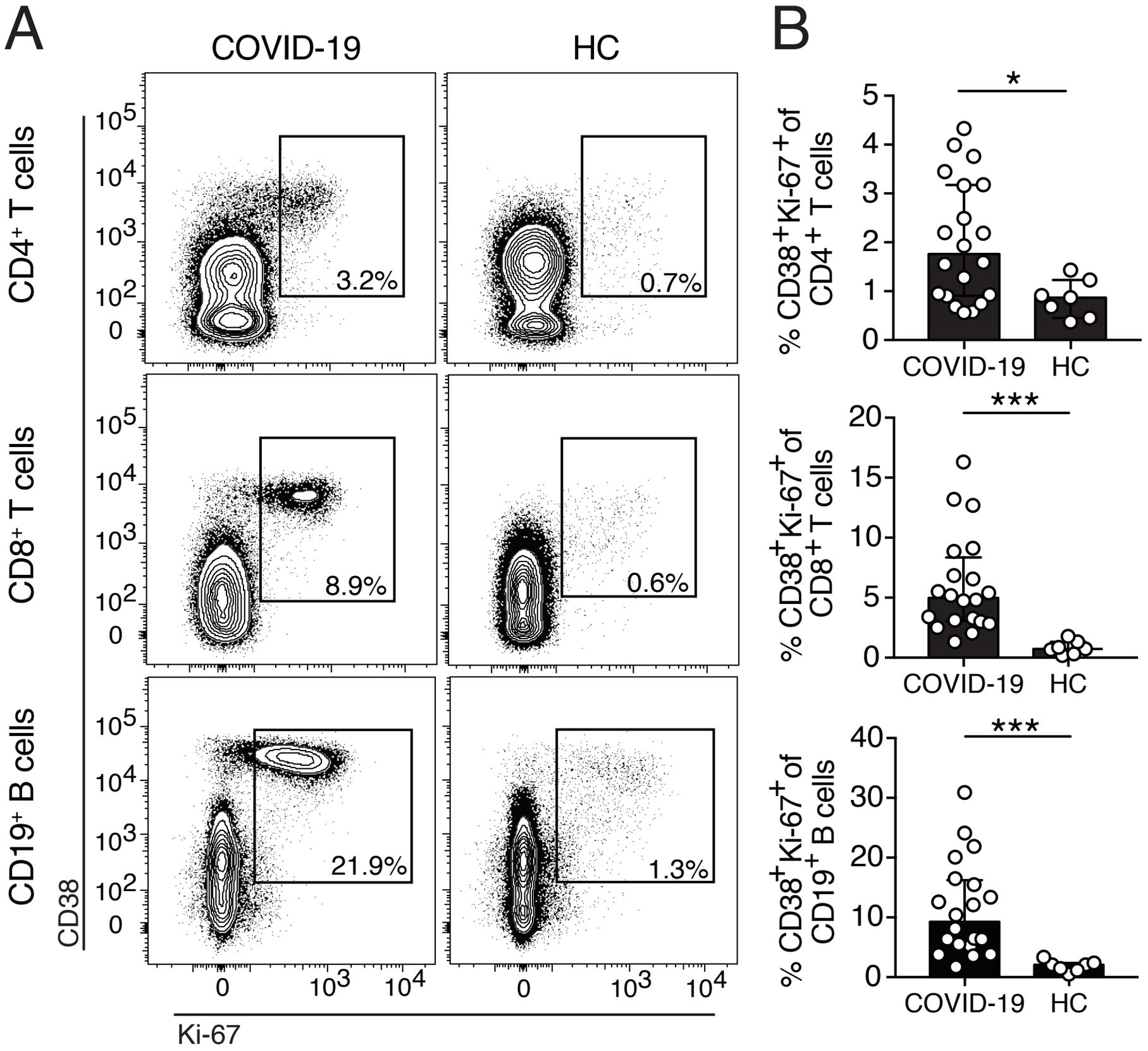

Figure 3 Varnaite et al.

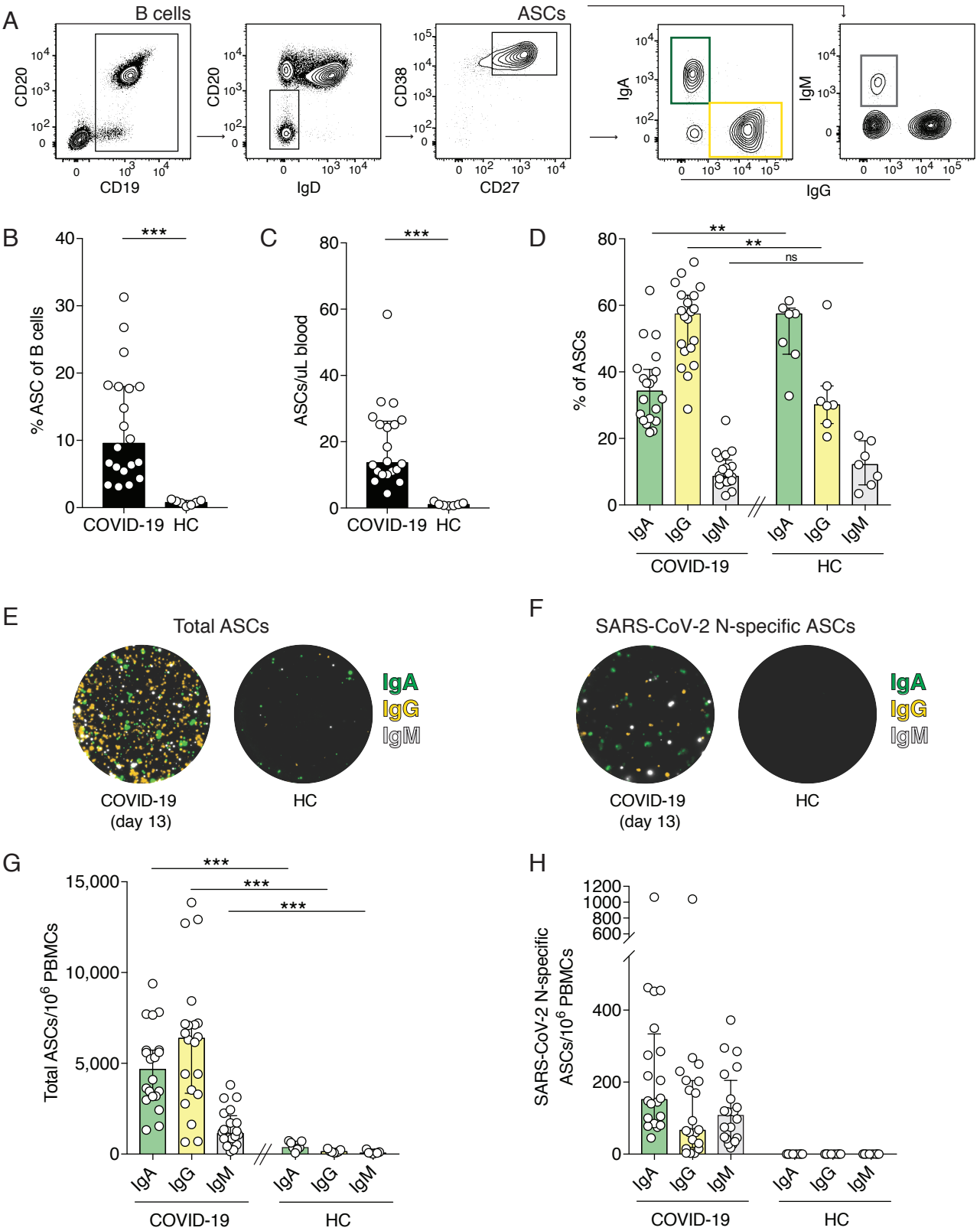

Figure 4 Varnaite et al.

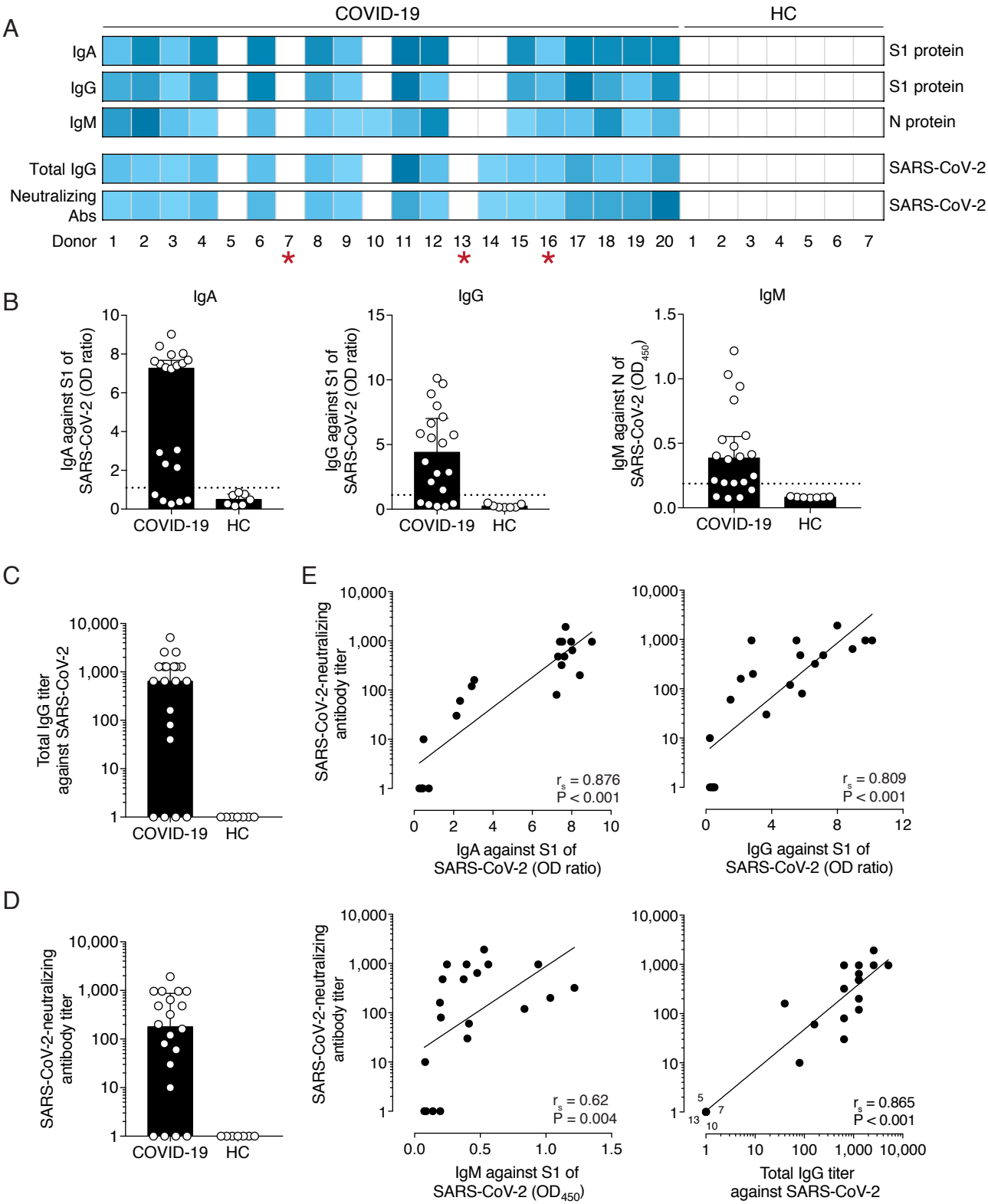

Figure 5 Varnaite et al.

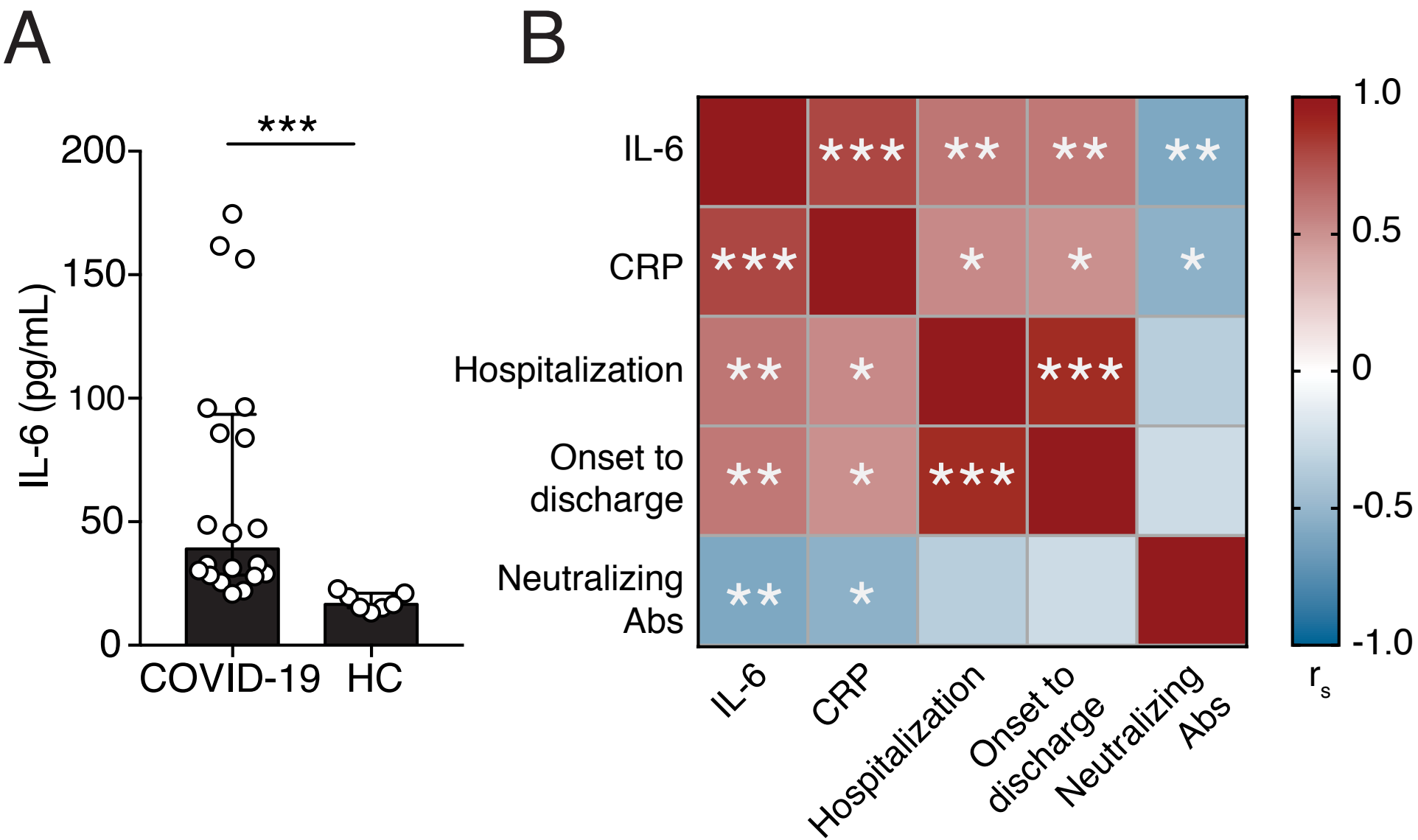

Supplementary Figure 1

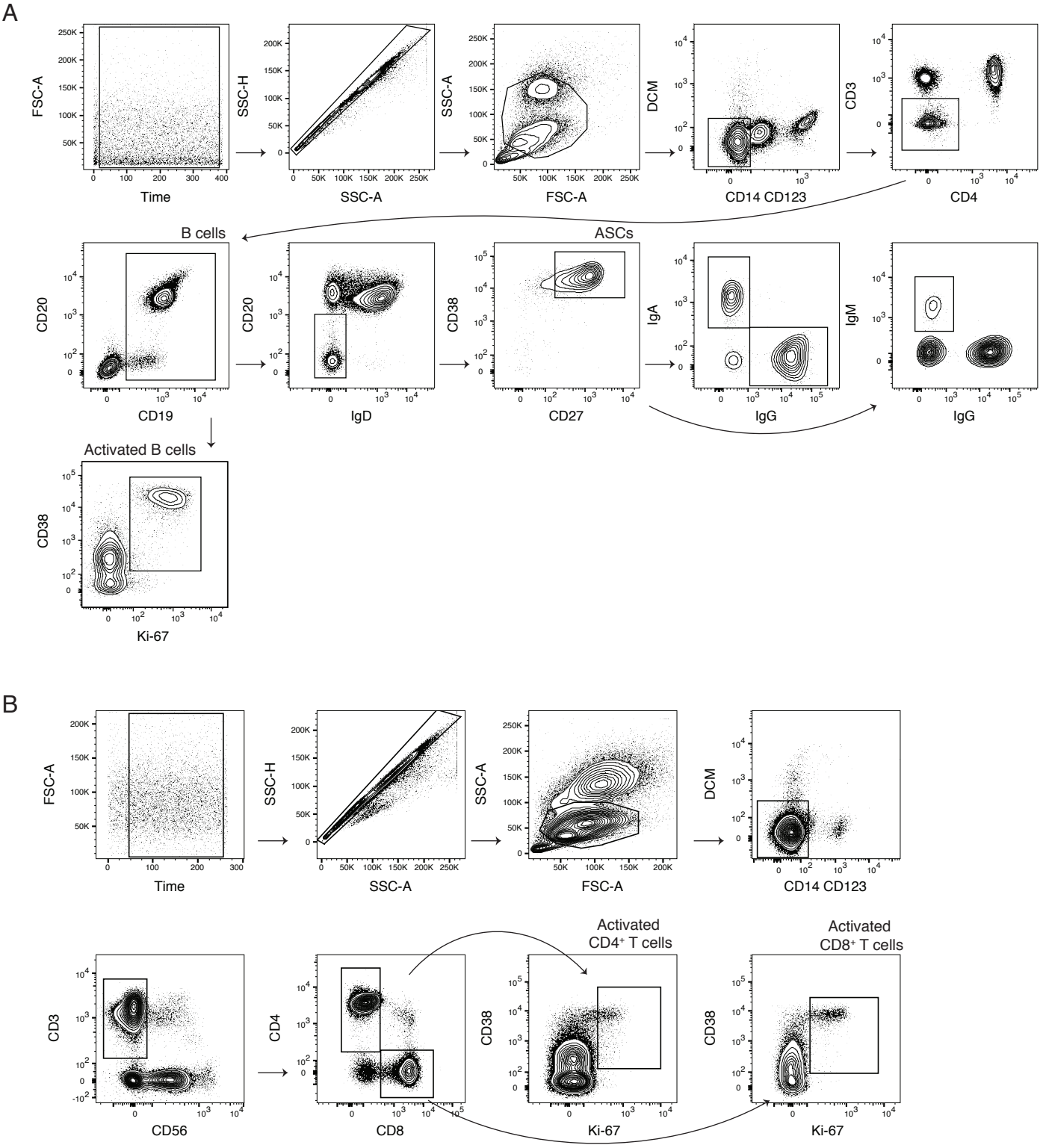

(A) Flow cytometry gating strategy for antibody-secreting cells (ASCs), the IgA, IgG and IgM ASC subsets, as well as activated B cells. (B) Flow cytometry gating strategy for $CD4^+$ and $CD8^+$ T cell activation, defined as the co-expression of CD38 and Ki-67.

Supplementary Figure 2

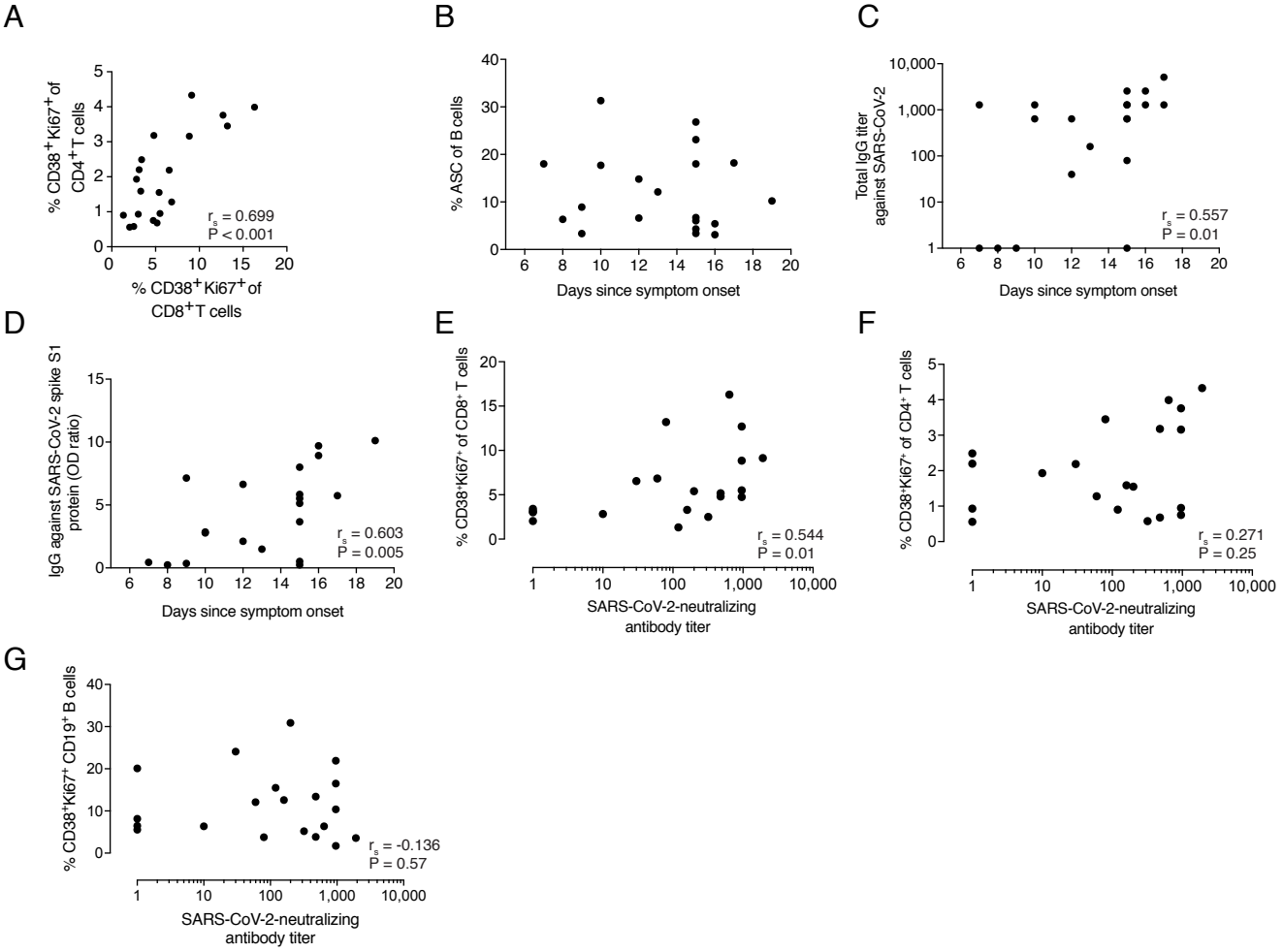

(A) Correlation between CD4+ and CD8+ T cell activation levels, as measured by CD38 and Ki-67 co-expression using flow cytometry. (B) Graph displaying the antibody-secreting cell (ASC) frequencies within the total pool of CD19+ B cells and the number of days since symptom onset of COVID-19. (C) Correlation between total IgG titers against SARS-CoV-2 (measured by IFA) and the number of days since symptom onset of COVID-19. (D) Correlation between levels of SARS-CoV-2 S1 protein-specific IgG levels and the number of days since symptom onset of COVID-19. (E-G) Correlations between activated T cells and B cells with SARS-CoV-2 neutralizing antibody titers. Correlations were examined by Spearman's correlation test. r_s: Spearman's rank correlation coefficient. $P < 0.05$ was considered statistically significant.